Pergamon

0956-7151(94)E0126-2

Acta metall. mater. Vol. 42, No. 10, pp. 3503–3513, 1994

0956-7151/94 $7.00 + 0.00

COMPUTER SIMULATION OF SPINODAL DECOMPOSITION IN TERNARY SYSTEMS

LONG-QING CHEN

Department of Materials Science and Engineering, Pennsylvania State University, University Park, PA 16802, U.S.A.

(Received 16 September 1993; in revised form 11 January 1994)

Abstract—The non-linear spinodal decomposition kinetics of a quenched homogeneous ternary alloy within three- or two-phase fields is modeled using a computer simulation technique formulated in the reciprocal lattice. Based on two-dimensional computer simulations, it is shown that, similar to binary alloys, spinodal decomposition in a ternary system usually produces interconnected morphologies at the very early stages of decomposition. For most of the compositions investigated, a decomposition of a homogeneous phase into three phases takes place in two stages. For some compositions, the two stages are the phase separation of an homogeneous phase into two phases, followed by further phase separation of one of the two phases into another two phases, resulting in a three-phase mixture. For other compositions, the first stage is a phase separation of an initially homogeneous phase into a two-phase mixture followed by a second stage, the appearance of a third phase along the existing interphase boundaries. This sequential phase separation in a ternary alloy can be justified from a thermodynamic stability analysis combined with the knowledge of the thermodynamic driving force for phase separation. It is also demonstrated that a third minor component strongly segregates to interphase boundaries during spinodal decomposition and subsequent coarsening of a homogeneous ternary alloy into two phases.

INTRODUCTION

A fundamental understanding of the kinetics of solid-state decomposition or precipitation reactions during an alloy aging is crucial for controlling microstructures and thus the properties of technologically important multi-phase materials. It is generally believed that, depending on the aging temperature and alloy composition within a two-phase field, there are two different modes of decomposition reactions in alloys. One proceeds through nucleation and growth of second phase precipitate particles which occurs when an initial homogenous phase is stable with respect to small compositional variations but unstable with respect to large ones. The other is spinodal decomposition which develops as a result of the loss of the intrinsic stability of a quenched homogeneous single-phase. Since the classical work of Cahn and Hilliard [1] and Cahn [2], there have been extensive experimental and theoretical works on the thermodynamics and kinetics of spinodal decomposition in binary systems and most of the early investigations were summarized in the 1969 paper of Hilliard [3]. However, there have been only a few investigations concerning decomposition reactions in ternary alloys despite the fact that the most technologically important alloys are multicomponent. Among these, most of the early works were mostly concerned with thermodynamic stability and phase diagrams of model ternary systems [4–8]. Only recently, nonlinear spinodal decomposition equations for the local composition and for the pair correlation functions in a ternary system were obtained [9] based on a non-linear kinetic theory derived from the Macroscopic Master Equations [10] and the very early stages of decomposition kinetics was analyzed by employing the linearized kinetic equations [11]. However, to the author's knowledge, the nonlinear dynamics of inhomogeneous morphological evolution during spinodal decomposition including the subsequent coarsening process in a ternary system has not been extensively investigated. Therefore, the main objective of this work is to model the microstructural evolution dynamics during spinodal decomposition in ternary alloys by numerically solving the non-linear microscopic diffusion equations [12]. To reach this objective, I will employ a computer simulation technique recently developed for ternary systems [13]. Due to the microscopic nature of the kinetic model, it can be applied to model either ordering or phase separation as well as simultaneous ordering and phase separation. Moreover, the coarsening kinetics of a two- or three-phase mixture of a ternary alloy can be easily modeled using this technique. In this paper, computer simulation of isostructural spinodal decomposition in a ternary alloy is performed for several representative compositions in a simple two-dimensional model system with a square lattice. Some important aspects of the decomposition reaction in ternary systems, which cannot be observed in binary systems, will be particularly emphasized. The microstructural evolution for

various modes of spinodal decomposition as well as the coarsening kinetics will be discussed by analyzing computer-generated morphological patterns.

THE KINETIC MODEL

Following [13], atomic structures and morphologies of a ternary alloy system are described by single-site occupation probability functions, $nv(\mathbf{r}, t)$, defined at each lattice site $\mathbf{r}$ for a given moment of time, t, where v denotes the kind of species in a ternary alloy. For instance, $n_A(\mathbf{r}, t)$ is the probability of finding A atoms at lattice site, $\mathbf{r}$, for a given moment of time, t, $n_B(\mathbf{r}, t)$ is the probability of finding B atoms at lattice site $\mathbf{r}$ for time t, and $n_C(\mathbf{r}, t)$ is the probability of finding C atoms at lattice site $\mathbf{r}$ for time t. At very high temperatures, the equilibrium state of a system corresponds to a homogeneous disordered state described by $n_v(\mathbf{r}, t) = c_v$ where c_v is the overall composition for component v. When such an homogeneous phase is quenched to low temperatures, it will become unstable with respect to atomic ordering, or compositional clustering, or both (I ignore the displacive transformations) depending on the interatomic interactions within the system. The evolution of the initially unstable state to a stable one is a highly nonlinear and complex process. It is assumed in this paper that such a process may be described by the Onsager-type microscopic diffusion equations which was first proposed by Khachaturyan [12]. Recent kinetic studies by the author and his coworkers indicated that those equations described adequately the sequence of diffusional phase transformations in binary alloys [14]. Since for ternary systems $n_A(\mathbf{r}, t) + n_B(\mathbf{r}, t) + n_C(\mathbf{r}, t) = 1.0$, only two equations are independent at each lattice site. If one assumes that the independent valuables are $n_A(\mathbf{r}, t)$ and $n_B(\mathbf{r}, t)$, there will be two independent kinetic equations at each lattice site for species A and B, respectively. Then, one can write the microscopic kinetic equations for ternary systems as

$$\frac{\mathrm{d}_A n(\mathbf{r}, t)}{\mathrm{d}t} = \frac{1}{k_B T}\sum_{\mathbf{r}'}\left[L_{AA}(\mathbf{r}-\mathbf{r}')\frac{\delta F}{\delta n_A(\mathbf{r}', t)} + L_{AB}(\mathbf{r}-\mathbf{r}')\frac{\delta F}{\delta n_B(\mathbf{r}', t)}\right]$$

and

$$\frac{\mathrm{d}n_B(\mathbf{r}, t)}{\mathrm{d}t} = \frac{1}{k_B T}\sum_{\mathbf{r}'}\left[L_{BA}(\mathbf{r}-\mathbf{r}')\frac{\delta F}{\delta n_A(\mathbf{r}', t)} + L_{BB}(\mathbf{r}-\mathbf{r}')\frac{\delta F}{\delta n_B(\mathbf{r}', t)}\right] \quad (1)$$

where $L_{v\mu}(\mathbf{r}-\mathbf{r}')$ are the exchange probabilities between a pair of atoms, v and μ, at lattice site $\mathbf{r}$ and $\mathbf{r}'$ within a time unit, and F is the total Helmholtz free energy of the system. In the single-site approximation, the free energy F for a ternary system is given by

$$\begin{aligned} F = -\frac{1}{2}\sum_{\mathbf{r}}\sum_{\mathbf{r}'}[&V_{AB}(\mathbf{r}-\mathbf{r}')n_A(\mathbf{r})n_B(\mathbf{r}') \\ &+ V_{BC}(\mathbf{r}-\mathbf{r}')n_B(\mathbf{r})n_C(\mathbf{r}') \\ &+ V_{AC}(\mathbf{r}-\mathbf{r}')n_A(\mathbf{r})n_C(\mathbf{r}')] \\ &+ k_B T\sum_{\mathbf{r}}[n_A(\mathbf{r})\ln(n_A(\mathbf{r})) \\ &+ n_B(\mathbf{r})\ln(n_B(\mathbf{r})) + n_C(\mathbf{r})\ln(n_C(\mathbf{r}))] \end{aligned}$$

where k_B is the Boltzmann constant, T is the temperature and

$$\begin{aligned} V_{AB}(\mathbf{r}-\mathbf{r}') &= W_{AA}(\mathbf{r}-\mathbf{r}') + W_{BB}(\mathbf{r}-\mathbf{r}') - 2W_{AB}(\mathbf{r}-\mathbf{r}') \\ V_{BC}(\mathbf{r}-\mathbf{r}') &= W_{BB}(\mathbf{r}-\mathbf{r}') + W_{CC}(\mathbf{r}-\mathbf{r}') - 2W_{BC}(\mathbf{r}-\mathbf{r}') \\ V_{AC}(\mathbf{r}-\mathbf{r}') &= W_{AA}(\mathbf{r}-\mathbf{r}') + W_{CC}(\mathbf{r}-\mathbf{r}') - 2W_{AC}(\mathbf{r}-\mathbf{r}') \end{aligned}$$

in which $W_{v\mu}(\mathbf{r}-\mathbf{r}')$ are the pairwise interaction energies between a pair of atoms, v (=A, B or C) and μ (=A, B or C), at lattice site $\mathbf{r}$ and $\mathbf{r}'$.

One can eliminate $n_C(\mathbf{r})$ in the free energy expression by substituting $n_C(\mathbf{r})$ with $1 - n_A(\mathbf{r}) - n_B(\mathbf{r})$ and ignoring terms which do not depend on the inhomogeneous distribution of single-site occupation probability functions

$$\begin{aligned} F = \frac{1}{2}\sum_{\mathbf{r}}\sum_{\mathbf{r}'}[&(-V_{AB}(\mathbf{r}-\mathbf{r}') + V_{BC}(\mathbf{r}-\mathbf{r}') \\ &+ V_{AC}(\mathbf{r}-\mathbf{r}'))n_A(\mathbf{r})n_B(\mathbf{r}') \\ &+ V_{AC}(\mathbf{r}-\mathbf{r}')n_A(\mathbf{r})n_A(\mathbf{r}') \\ &+ V_{BC}(\mathbf{r}-\mathbf{r}')n_B(\mathbf{r})n_B(\mathbf{r}')] \\ &+ k_B T\sum_{\mathbf{r}}[n_A(\mathbf{r})\ln(n_A(\mathbf{r})) \\ &+ n_B(\mathbf{r})\ln(n_B(\mathbf{r})) + (1 - n_A(\mathbf{r}) \\ &- n_B(\mathbf{r}))\ln(1 - n_A(\mathbf{r}) - n_B(\mathbf{r}))]. \end{aligned} \quad (2)$$

The variational derivatives in the kinetic equation (1) can, then, be written as

$$\begin{aligned} \frac{\delta F}{\delta n_A(\mathbf{r}')} = \frac{1}{2}\sum_{\mathbf{r}}[&(-V_{AB}(\mathbf{r}-\mathbf{r}') + V_{BC}(\mathbf{r}-\mathbf{r}') \\ &+ V_{AC}(\mathbf{r}-\mathbf{r}'))]n_B(\mathbf{r}) \\ &+ \sum_{\mathbf{r}} V_{AC}(\mathbf{r}-\mathbf{r}')n_A(\mathbf{r}) \\ &+ k_B T\ln\left[\frac{n_A(\mathbf{r}')}{(1 - n_A(\mathbf{r}') - n_B(\mathbf{r}'))}\right] \end{aligned}$$

and

$$\frac{\delta F}{\delta n_B(\mathbf{r}')} = \frac{1}{2}\sum_{\mathbf{r}}[(-V_{AB}(\mathbf{r}-\mathbf{r}') + V_{BC}(\mathbf{r}-\mathbf{r}') + V_{AC}(\mathbf{r}-\mathbf{r}'))]n_A(\mathbf{r}) + \sum_{\mathbf{r}} V_{BC}(\mathbf{r}-\mathbf{r}')n_B(\mathbf{r}) + k_B T \ln\left[\frac{n_B(\mathbf{r}')}{(1-n_A(\mathbf{r}')-n_B(\mathbf{r}'))}\right]. \quad (3)$$

Since the total number of A, B and C atoms are fixed, one has the condition

$$\sum_{\mathbf{r}} \frac{dn_v(\mathbf{r})}{dt} = \frac{dN_v}{dt} = 0 \quad (4)$$

where N_v is the total number of v (= A, B or C) atoms in the system. Equation (4) implies that

$$\sum_{\mathbf{r}} L_{v\mu}(\mathbf{r}) = 0, \quad v, \mu = \text{A or B}. \quad (5)$$

Fourier transform of the kinetic equations (1) with the variational derivatives (3) gives

$$\frac{d\tilde{n}_A(\mathbf{k},t)}{dt} = \frac{\tilde{L}_{AA}(\mathbf{k})}{k_B T}\left\{\tilde{V}_{AC}(\mathbf{k})\tilde{n}_A(\mathbf{k},t) + \tfrac{1}{2}[-\tilde{V}_{AB}(\mathbf{k}) + \tilde{V}_{BC}(\mathbf{k}) + \tilde{V}_{AC}(\mathbf{k})]\tilde{n}_B(\mathbf{k},t) + k_B T\left\{\ln\left[\frac{n_A(\mathbf{r},t)}{(1-n_A(\mathbf{r},t)-n_B(\mathbf{r},t))}\right]\right\}_{\mathbf{k}}\right\} + \tilde{L}_{AB}(\mathbf{k})\left\{\tilde{V}_{BC}(\mathbf{k})\tilde{n}_B(\mathbf{k},t) + \tfrac{1}{2}[-\tilde{V}_{AB}(\mathbf{k}) + \tilde{V}_{BC}(\mathbf{k}) + \tilde{V}_{AC}(\mathbf{k})]\tilde{n}_A(\mathbf{k},t) + k_B T\left\{\ln\left[\frac{n_B(\mathbf{r},t)}{(1-n_A(\mathbf{r},t)-n_B(\mathbf{r},t))}\right]\right\}_{\mathbf{k}}\right\}$$

and

$$\frac{d\tilde{n}_B(\mathbf{k},t)}{dt} = \frac{\tilde{L}_{BA}(\mathbf{k})}{k_B T}\left\{\tilde{V}_{AC}(\mathbf{k})\tilde{n}_A(\mathbf{k},t) + \tfrac{1}{2}[-\tilde{V}_{AB}(\mathbf{k}) + \tilde{V}_{BC}(\mathbf{k}) + \tilde{V}_{AC}(\mathbf{k})]\tilde{n}_B(\mathbf{k},t) + k_B T\left\{\ln\left[\frac{n_A(\mathbf{r},t)}{(1-n_A(\mathbf{r},t)-n_B(\mathbf{r},t))}\right]\right\}_{\mathbf{k}}\right\} + \tilde{L}_{BB}(\mathbf{k})\left\{\tilde{V}_{BC}(\mathbf{k})\tilde{n}_B(\mathbf{k},t) + \tfrac{1}{2}[-\tilde{V}_{AB}(\mathbf{k}) + \tilde{V}_{BC}(\mathbf{k}) + \tilde{V}_{AC}(\mathbf{k})]\tilde{n}_A(\mathbf{k},t) + k_B T\left\{\ln\left[\frac{n_B(\mathbf{r},t)}{(1-n_A(\mathbf{r},t)-n_B(\mathbf{r},t))}\right]\right\}_{\mathbf{k}}\right\} \quad (6)$$

where $\tilde{n}_A(\mathbf{k},t)$, $\tilde{n}_B(\mathbf{k},t)$, $\{\ln[n_A(\mathbf{r},t)/(1-n_A(\mathbf{r},t)-n_B(\mathbf{r},t))]\}_{\mathbf{k}}$, $\{\ln[n_B(\mathbf{r},t)/(1-n_A(\mathbf{r},t)-n_B(\mathbf{r},t))]\}_{\mathbf{k}}$, $\tilde{V}_{AB}(\mathbf{k})$, $\tilde{V}_{BC}(\mathbf{k})$, $\tilde{V}_{AC}(\mathbf{k})$, $\tilde{L}_{AA}(\mathbf{k})$, $\tilde{L}_{AB}(\mathbf{k})$, $\tilde{L}_{BA}(\mathbf{k})$, and $\tilde{L}_{BB}(\mathbf{k})$ are Fourier transforms of corresponding functions in the real space. Under the assumption of atomic exchange between nearest neighbor sites only and the condition that the total number of atoms is conserved [equations (4) and (5)], the Fourier transform of the L-matrix can be calculated as follows Since

$$\sum_{\mathbf{r}} L_{v\mu}(\mathbf{r}) = L_{v\mu}(0) + \sum_{\mathbf{r}}' L_{v\mu}(\mathbf{r}) = 0,$$

one has

$$\tilde{L}_{v\mu}(\mathbf{k}) = \sum_{\mathbf{r}} L_{v\mu}(\mathbf{r})e^{-i\mathbf{k}\mathbf{r}} = -\sum_{\mathbf{r}}' L_{v\mu}(\mathbf{r})(1-e^{-i\mathbf{k}\mathbf{r}}) = -2\sum_{\mathbf{r}}' L_{v\mu}(\mathbf{r})\sin^2(\tfrac{1}{2}\mathbf{k}\mathbf{r}) \quad (7)$$

where the summations are over all nearest-neighbor sites $\mathbf{r}$ and prime in the summation indicates that $\mathbf{r} = 0$ term is omitted.

The computer simulation is performed through a numerical solution of kinetic equation (6), given initial single-site occupation probability distribution and interatomic interactions.

THE INSTABILITY SURFACE FOR A TERNARY SYSTEM (T–c INSTABILITY DIAGRAM)

At equilibrium, by definition, the variational derivatives of the total Helmholtz free energy with respect to the occupation probabilities should be zero, i.e.

$$\frac{\delta F}{\delta n_A(\mathbf{r}')} = 0 \quad \text{and} \quad \frac{\delta F}{\delta n_B(\mathbf{r}')} = 0. \quad (8)$$

At high temperatures, the equilibrium state for a ternary alloy is a homogeneous disordered state. Therefore, at high temperatures, $n_A(\mathbf{r}) = c_A$ and $n_B(\mathbf{r}) = c_B$ is the solution to equation (8). At low temperatures, let us examine the solution, $n_A(\mathbf{r}) = c_A + \delta n_A(\mathbf{r})$ and $n_B(\mathbf{r}) = c_B + \delta n_B(\mathbf{r})$. Using the expressions for the variational derivatives in equation (3) and expanding them to the first order of $\delta n_A(\mathbf{r})$ and $\delta n_B(\mathbf{r})$, one gets

$$\frac{1}{2}\sum_{\mathbf{r}}[-V_{AB}(\mathbf{r}-\mathbf{r}') + V_{BC}(\mathbf{r}-\mathbf{r}') + V_{AC}(\mathbf{r}-\mathbf{r}')]\delta n_B(\mathbf{r}) + \sum_{\mathbf{r}} V_{AC}(\mathbf{r}-\mathbf{r}')\delta n_A(\mathbf{r}) + k_B T\left[\frac{1}{c_A}+\frac{1}{c_C}\right]\delta n_A(\mathbf{r}') + \frac{k_B T}{c_C}\delta n_B(\mathbf{r}') = 0$$

and

$$\frac{1}{2}\sum_{\mathbf{r}}[-V_{AB}(\mathbf{r}-\mathbf{r}') + V_{BC}(\mathbf{r}-\mathbf{r}') + V_{AC}(\mathbf{r}-\mathbf{r}')]\delta n_A(\mathbf{r}) + \sum_{\mathbf{r}} V_{BC}(\mathbf{r}-\mathbf{r}')\delta n_B(\mathbf{r}) + k_B T\left[\frac{1}{c_A}+\frac{1}{c_C}\right]\delta n_B(\mathbf{r}') + \frac{k_B T}{c_C}\delta n_A(\mathbf{r}') = 0. \quad (9)$$

Fourier transforming these two equations into reciprocal space, one has

$$\tfrac{1}{2}[-\tilde{V}_{AB}(\mathbf{k})+\tilde{V}_{BC}(\mathbf{k})+\tilde{V}_{AC}(\mathbf{k})]\delta\tilde{n}_B(\mathbf{k}) + \tilde{V}_{AC}(\mathbf{k})\delta\tilde{n}_A(\mathbf{k})+k_BT\left[\frac{1}{c_A}+\frac{1}{c_C}\right]\delta\tilde{n}_A(\mathbf{k}) + \frac{k_BT}{c_C}\delta\tilde{n}_B(\mathbf{k})=0$$

and

$$\tfrac{1}{2}[-\tilde{V}_{AB}(\mathbf{k})+\tilde{V}_{BC}(\mathbf{k})+\tilde{V}_{AC}(\mathbf{k})]\delta\tilde{n}_A(\mathbf{k}) + \tilde{V}_{BC}(\mathbf{k})\delta\tilde{n}_B(\mathbf{k})+k_BT\left[\frac{1}{c_B}+\frac{1}{c_C}\right]\delta\tilde{n}_A(\mathbf{k}) + \frac{k_BT}{c_C}\delta\tilde{n}_A(\mathbf{k})=0. \quad (10)$$

Nontrivial solutions for $\delta\tilde{n}_A(\mathbf{k})$ and $\delta\tilde{n}_B(\mathbf{k})$ exist when

$$\begin{vmatrix} \tilde{V}_{AC}(\mathbf{k})+k_BT\left(\frac{1}{c_A}+\frac{1}{c_C}\right), & \tfrac{1}{2}[-\tilde{V}_{AB}(\mathbf{k})+\tilde{V}_{BC}(\mathbf{k})+\tilde{V}_{AC}(\mathbf{k})]+\frac{k_BT}{c_C} \\ \tfrac{1}{2}[-\tilde{V}_{AB}(\mathbf{k})+\tilde{V}_{BC}(\mathbf{k})+\tilde{V}_{AC}(\mathbf{k})]+\frac{k_BT}{c_C}, & \tilde{V}_{BC}(\mathbf{k})+k_BT\left(\frac{1}{c_B}+\frac{1}{c_C}\right) \end{vmatrix} = 0 \quad (11)$$

which defines the instability surface of the original homogeneous disordered alloy with respect to the growth of concentration wave amplitudes, $\delta\tilde{n}_A(\mathbf{k})$ and $\delta\tilde{n}_B(\mathbf{k})$. Expanding the above determinant, one obtains the equation

$$(k_BT)^2+k_BT[\tilde{V}_{BC}(\mathbf{k})c_Bc_C+\tilde{V}_{AC}(\mathbf{k})c_Ac_C + \tilde{V}_{AB}(\mathbf{k})c_Ac_B]+\tilde{V}_{AC}(\mathbf{k})\tilde{V}_{BC}(\mathbf{k})c_Ac_Bc_C - \tfrac{1}{4}[-\tilde{V}_{AB}(\mathbf{k})+\tilde{V}_{AC}(\mathbf{k}) + \tilde{V}_{BC}(\mathbf{k})]^2c_Ac_Bc_C=0 \quad (12)$$

where c_A, c_B and c_C are average compositions for component A, B and C, respectively. The same result was obtained in [7].

When $c_C=0$, it is reduced to the binary case

$$k_BT=-c_Ac_B\tilde{V}_{AB}(\mathbf{k}).$$

The limit of stability for spinodal decomposition corresponds to $\mathbf{k}=0$. Therefore, the spinodal surface is given by

$$(k_BT)^2+k_BT[\tilde{V}_{BC}(0)c_Bc_C+\tilde{V}_{AC}(0)c_Ac_C + \tilde{V}_{AB}(0)c_Ac_B] + \tilde{V}_{AC}(0)\tilde{V}_{BC}(0)c_Ac_Bc_C - \tfrac{1}{4}[-\tilde{V}_{AB}(0)+\tilde{V}_{AC}(0)+\tilde{V}_{BC}(0)]^2c_Ac_Bc_C=0. \quad (13)$$

Assume the symmetric case where $\tilde{V}_{AB}(0)=\tilde{V}_{BC}(0)=\tilde{V}_{AC}(0)=\tilde{V}(0)<0$, then

$$(k_BT)^2+k_BT[c_Bc_C+c_Ac_C+c_Ac_B]\tilde{V}(0) + \tfrac{3}{4}\tilde{V}^2(0)c_Ac_Bc_c=0. \quad (14)$$

Let $k_BT/|\tilde{V}(0)|=\tau$, one has

$$\tau^2-(c_Ac_B+c_Ac_C+c_Bc_C)\tau+\tfrac{3}{4}c_Ac_Bc_C=0. \quad (15)$$

The solutions to (13) are

$$\tau_\pm=\frac{(c_Ac_B+c_Ac_C+c_Bc_C)\pm\sqrt{(c_Ac_B+c_Ac_C+c_Bc_C)^2-3c_Ac_Bc_C}}{2}. \quad (16)$$

If $c_C=0$, $\tau_+=c_Ac_B$, $\tau_-=0$ (binary case).

Let us look at some particular alloys in which the compositions for A and B are equal, i.e. $c_A=c_B=c$, then

$$c_C=1-c_A-c_B=1-2c.$$

Substituting these relations into equation (16), one obtains

$$\tau_+=\tfrac{3}{2}c(1-2c) \quad \text{and} \quad \tau_-=\frac{c}{2} \quad (17)$$

where τ_+ and τ_- correspond to two branches of the instability surface of a ternary alloy along the composition space in which $c_A=c_B$.

COMPUTER SIMULATION RESULTS AND DISCUSSIONS

As an example, we employ a two-dimensional square lattice to study the spinodal decomposition kinetics of a homogeneous disordered ternary alloy into a three- or two-phase mixture of disordered phases.

To obtain spinodal decomposition in ternary alloys, it is sufficient to assume nearest neighbor interaction only. In particular, I chose the following interaction parameters

$$W_{AB}=-1.0; \quad W_{BC}=-1.0; \quad W_{AC}=-1.0. \quad (18)$$

It is emphasized that the computer simulation technique formulated in previous sections is valid for any range of interactions. Moreover, since the kinetic equations are solved in the reciprocal space, the computation time required for a system with a long-range interaction will be the same as those with short-range interactions. For a two-dimensional square lattice, the Fourier transform of W_{AB}, W_{BC} and W_{AC} are given by

$$\tilde{V}_{AB}(\mathbf{k})=2W_{AB}[\cos 2\pi h+\cos 2\pi l]$$

$$\tilde{V}_{BC}(\mathbf{k})=2W_{BC}[\cos 2\pi h+\cos 2\pi l]$$

$$\tilde{V}_{AC}(\mathbf{k})=2W_{AC}[\cos 2\pi h+\cos 2\pi l]$$

where h and l are related to the reciprocal lattice vector by $\mathbf{k}=2\pi/a_0(h\mathbf{i}+l\mathbf{j})$ in which a_0 is the lattice parameter of the real space square lattice, $\mathbf{i}$ and $\mathbf{j}$ are the unit vectors along the two-dimensional Cartesian coordinate axes.

An isothermal section of the phase diagram derived from the set of interaction parameters (18) and the free energy model (2) is shown in Fig. 1. It is calculated by using Kikuchi's Natural Iteration Method (NIM) [5]. In the diagram, the A-rich phase is labeled as α, B-rich phase as β and the C-rich phase as γ. The temperature for this phase diagram is chosen to be $k_B T = 0.4$, or in reduced unit, $\tau = k_B T/\tilde{V}(0) = 0.1$. All the following computer simulations were performed at the reduced temperature $\tau = 0.1$. At temperature $\tau = 0.1$, the equilibrium compositions of α, β and γ phases in a three-phase mixture are ($c_A = 0.9852$, $c_B = 0.0074$, $c_C = 0.0074$), ($c_A = 0.0074$, $c_B = 0.9852$, $c_C = 0.0074$) and ($c_A = 0.0074$, $c_B = 0.0074$, $c_C = 0.9852$), respectively.

The spinodal instability surface sectioned at $\tau = 0.1$ is schematically shown in Fig. 2. In region I, both eigenvalues of the matrix formed by the second derivatives (F''_{xy}, where F is the free energy, x, $y = c_A$ or c_B, and the double prime represents second derivative) of the free energy with respect to c_A and c_B are negative and therefore alloys with region I are unstable with respect to composition fluctuations along any directions in the composition space or called the negative definite region. In region II, only one of the eigenvaues is negative and alloys within region II are unstable only along certain directions in the ternary composition triangle or called the positive indefinite region. Alloy within region III are stable with respect to any small compositional fluctuations and spinodal decomposition is impossible in this region or it is called the positive definite region.

The compositions which are considered in the computer simulation are chosen to be along the line C–d shown in Fig. 2. The inability surface along this line is shown in Fig. 3 where $c = c_A = c_B$ and $c_C = 1 - 2c$. The straight line corresponds to the

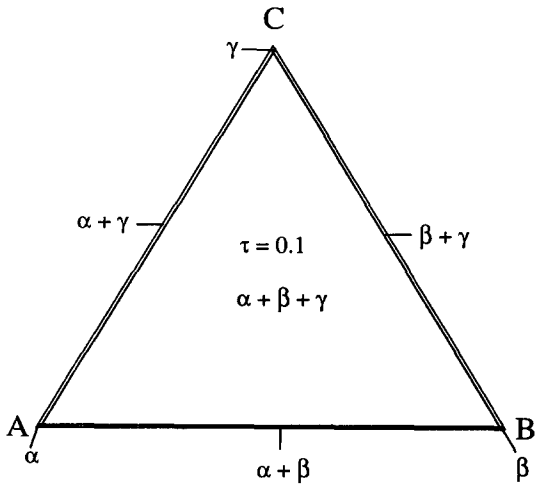

Fig. 1. An isothermal section of the ternary phase diagram calculated from the set of interaction parameters given in equation (18). α, β and γ are single-phase fields, $\alpha + \beta$, $\beta + \gamma$, and $\alpha + \gamma$ are two-phase fields, $\alpha + \beta + \gamma$ is the three-phase field.

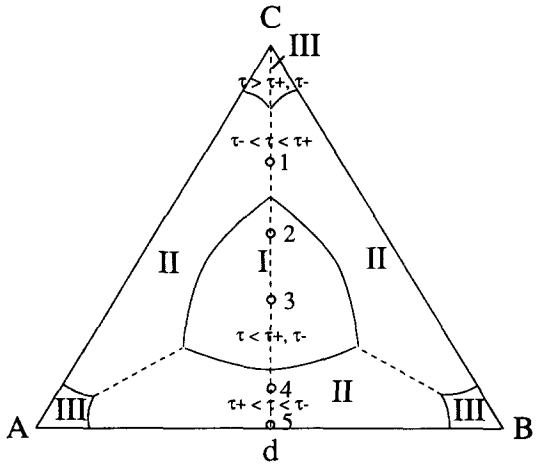

Fig. 2. An isothermal section of the spinodal instability surface at $\tau = 0.1$. I and II represent regions in which an alloy is unstable along any direction and a limited range of composition directions, respectively, in the composition space. III represents stable regions.

solution $\tau = c/2$ and the parabolic line corresponds to $\tau = (3/2)c(1 - 2c)$ in equation (17). As shown in Figs 2 and 3, systems with composition 3 and 4 at $\tau = 0.1$ are located below both the straight and parabolic instability lines ($\tau \leqslant \tau+, \tau-$) and therefore they are all-round unstable as defined by Meijering [4]. For composition 1, the system is initially unstable with respect to the decomposition along the direction C–d ($\tau_- < \tau < \tau_+$) while for compositions 4 and 5, the systems are initially unstable with respect to the decomposition along the direction parallel to A–B ($\tau_+ < \tau < \tau_-$). In the region where $\tau > \tau_+, \tau_-$ in Fig. 2, no spinodal decomposition is expected.

I chose the following coefficients for the L-matrix, $L_{\nu\mu}$, (arbitrarily chosen with the condition that it has to be positive definite) as

$$\begin{vmatrix} 1 & -1/2 & -1/2 \\ -1/2 & 1 & -1/2 \\ -1/2 & -1/2 & 1 \end{vmatrix}.$$

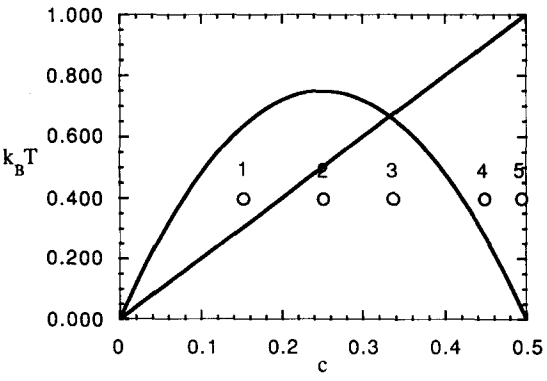

Fig. 3. The instability surface along the line C–d.

Employing equation (7), $\tilde{L}_{\nu\mu}(\mathbf{k})$ for a two-dimensional square lattice is given by

$$\tilde{L}_{\nu\mu}(\mathbf{k}) = -L_{\nu\mu}[2 - \cos 2\pi h - \cos 2\pi l]. \quad (19)$$

In the computer simulation, the kinetic equations are solved using the Euler technique

$$\tilde{n}_\nu(\mathbf{k}, t + \Delta t) = \tilde{n}_\nu(\mathbf{k}, t) + \frac{\mathrm{d}\tilde{n}_\nu(\mathbf{k}, t)}{\mathrm{d}t}\Delta t. \quad (20)$$

The size of the time step for integration, Δt, in the above equation is 0.005. The time is expressed in terms of a reduced time, i.e. $t^* = L_{AA}t$ where t is the real time and L_{AA} is the exchange probability between A atoms at nearest neighbor sites at a time unit. The initial state corresponds to a completely disordered state with uniform occupation probabilities at each lattice site. The maximum amplitude of the random perturbation to the initially completely disordered state is 0.005. Since we solve the kinetic equations in the reciprocal space, periodic boundary conditions are implied.

The morphological evolutions predicted from the computer simulations for four compositions, 1, 2, 4 and 5, shown in Figs 2 and 3 are exhibited in Figs 4–7. The morphological evolution for composition 3 has been published previously [13]. In those figures represented by black-and-white, the local composition profile is represented by gray-levels; the brighter the gray-level, the higher a local composition. Column $n_A(\mathbf{r}, t)$ represents the time evolution of the concentration profile of component A, column $n_B(\mathbf{r}, t)$ represents component B and column $n_C(\mathbf{r}, t)$ represents component C. In the color figures, the red color represents the α phase, the green color represents the β phase and the blue color represents the γ phase. For example, color levels from completely white to completely red represent c_A from 0.0 to 1.0 and the same representation applies to β and γ phase.

Composition 1: $c = c_A = c_B = 0.15$; $c_C = 0.70$

The morphological evolution for this composition is shown in Fig. 4. The initial stage decomposition is similar to that in binary systems; composition modulations with regions rich in C and with regions rich in both A and B (almost equal amount of A and B) develop from an initially homogeneous phase. At reduced time $t^* = 10$, a careful examination of the morphology shows that it is more or less interconnected even though one can hardly see any morphology in the printed picture in Fig. 4. As the decomposition proceeds, the A and B rich regions disconnect themselves into isolated regions ($t^* = 25$) which is still a two-phase morphology. The results indicates that the initial decomposition takes place primarily along the direction C–d in Fig. 2, which is consistent with the stability analysis as the system is above the linear instability line and below the parabolic instability line in Fig. 3. Although initial decomposition is mostly along the C–d direction, the instability along the A–B direction eventually developed in the A and B rich regions as C atoms continue to be depleted from those regions. We call the decomposition of the A–B rich regions into A-rich and B-rich regions as secondary decompositions. It results in the appearance of both α and β phase particles. It is interesting to point out that the secondary decomposition occurs almost exclusively within the A- and B-rich particles and it is expected that spinodal decomposition in very small grains in a polycrystalline solid might be very similar to what is observed in this simulation. Most of the A- and B-rich particles first decompose to approximately half α phase and half β phase. Different particles in the system decompose at slightly different times. Since simultaneous coarsening takes place during decomposition, some of the particles still contain half α and half β while others have become either completely α phase or completely β phase (see $t^* = 50$). The decomposed morphology consists of α and β phase particles embedded in a continuous matrix. During further coarsening, some of isolated α and β phase particles may coalesce to form a large particle with roughly half α and half β as it can be seen in Fig. 4 for $t^* = 100$.

Composition 2: $c = c_A = c_B = 0.25$; $c_C = 0.5$

In this case, the system is below both the straight instability line and the parabolic instability line and it is expected compositional modulations should develop along all directions. However, the driving force for decomposition along the C–d direction is larger than that along the direction A–B for this composition as it is shown in Fig. 3. Therefore, at short times, decomposition is primarily along the C–d direction as demonstrated in Fig. 5 that morphology is an interconnected two-phase mixture at time, $t^* = 10$. At a later time, the secondary decomposition of the interconnected A and B rich regions into A-rich and B-rich regions results in discrete α and β phase particles as shown in Fig. 5 for $t^* = 25$. Even after long-time annealing, the α and β phase particles form a beautiful bamboo-like structure. The γ phase is interconnected as it can be expected from the volume fraction which is about 50%.

Composition 4: $c = c_A = c_B = 0.45$; $c_C = 0.10$

The initial decomposition is primarily along the A–B direction and the C atoms segregate to the interphase boundaries between the α and β phases as shown in Fig. 6. This is again consistent with the instability surface shown in Figs 2 and 3 because composition 4 is above the parabolic instability line but below the linear instability line. Later discrete particles appear along the α/β interphase boundaries by barrierless nucleation and growth (see Fig. 6 for $t^* = 20$). If the precipitation of γ particles involves nucleation barrier, then they would not appear since in the present computer simulation technique the total free energy always decreases during the

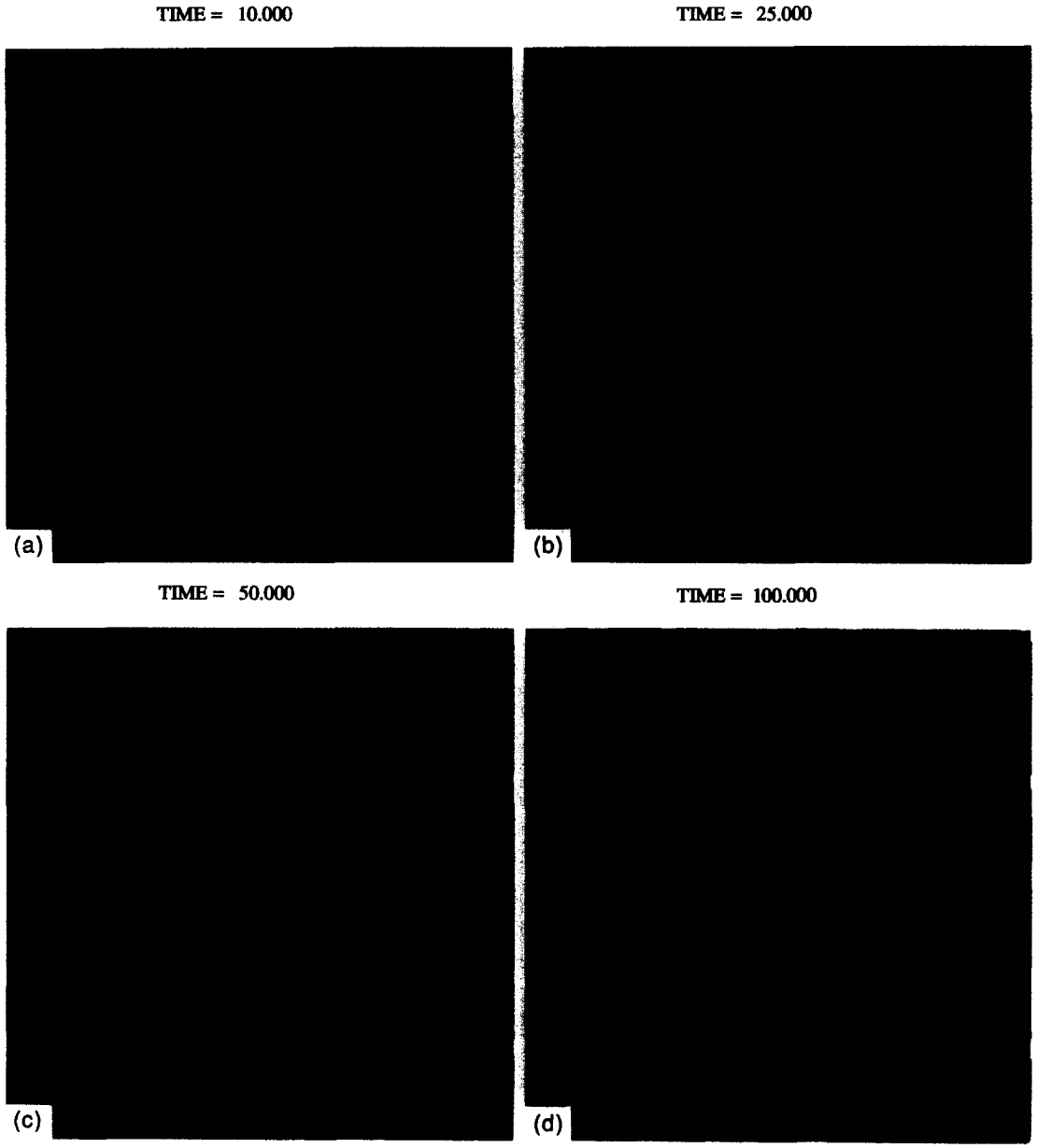

Fig. 4. Temporal evolution of morphologies during a spinodal phase separation of a ternary alloy with average composition $c_A = 0.15$, $c_B = 0.15$ and $c_C = 0.70$.

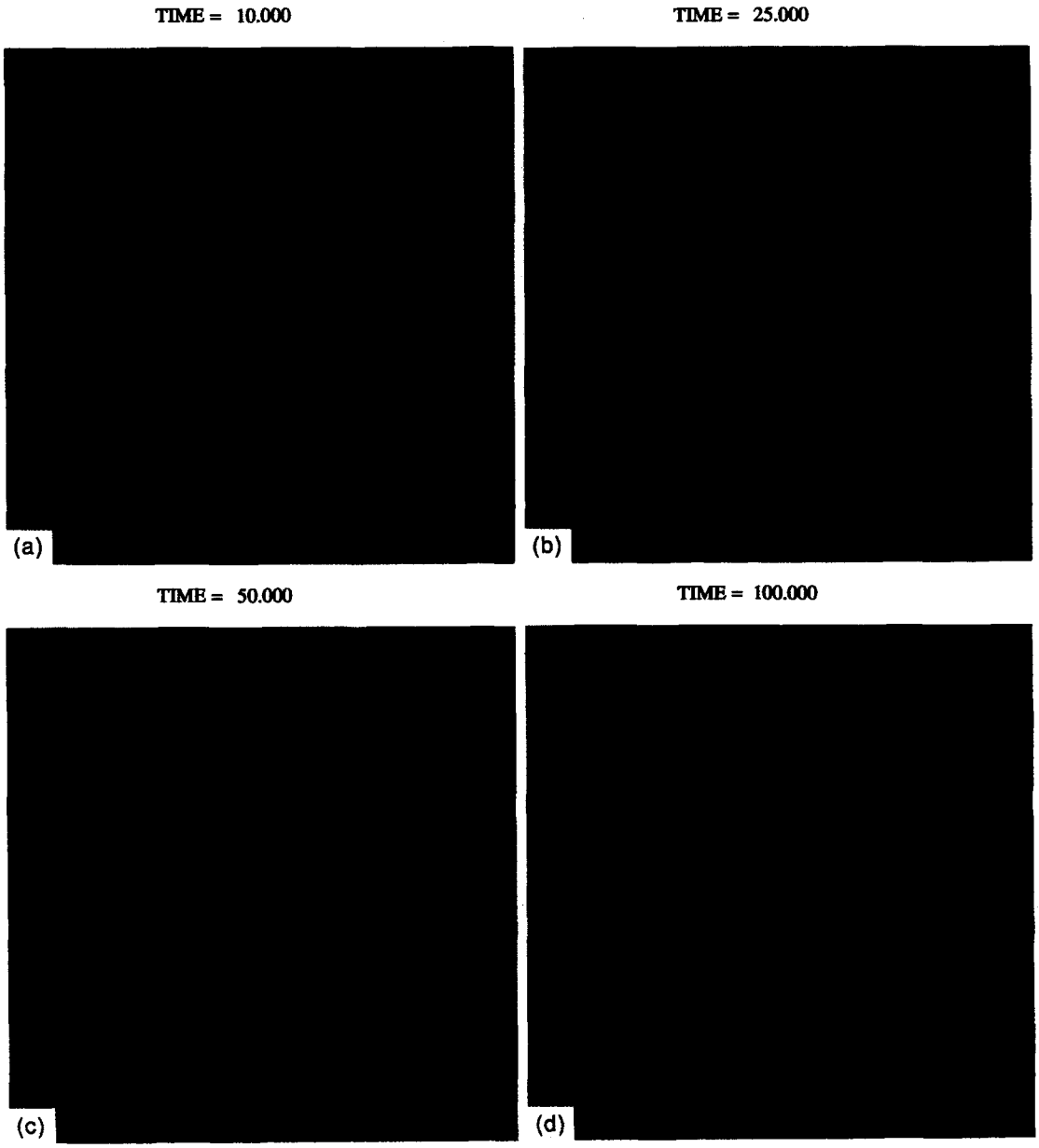

Fig. 5. Temporal evolution of morphologies during a spinodal phase separation of a ternary alloy with average composition $c_A = 0.25$, $c_B = 0.25$ and $c_C = 0.50$.

morphology evolution. In other words, the present technique can not describe activated process. The decomposed morphologies shown in Fig. 6 for $t^* = 50$ and 100 are interconnected structures of continuous α and β phases with γ phase particles sitting on the α/β interphase boundaries.

Composition 5: $c = c_A = c_B = 0.495$; $c_C = 0.01$

Spinodal decomposition for this composition is very similar to the spinodal decomposition with a 50–50% composition with interconnected morphologies in binary alloys. However, in this ternary case, the minor component C strongly segregates to the α/β interphase boundaries. The composition of C at the boundaries are about 6 times higher than that within the α and β composition domains (the composition of component C at the interphase boundaries is about 0.03 whereas the composition of component C inside the α and β particles is about 0.005). This segregation profile moves as the α/β two-phase mixture coarsens (Fig. 7). As a result of segregation, even though the overall average composition of this alloy falls within the three-phase region but near to the phase boundary, the composition inside the α and

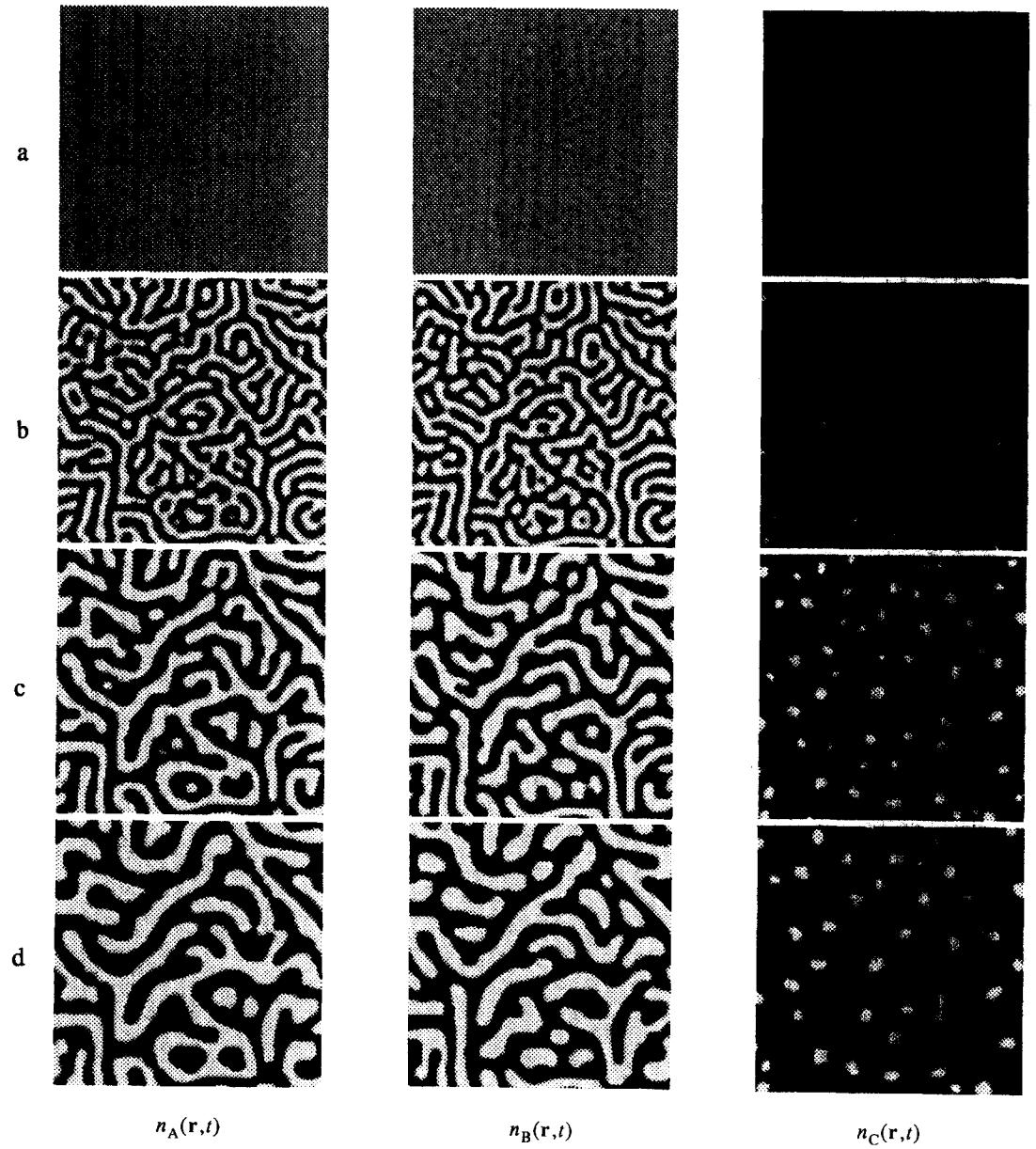

Fig. 6. Temporal evolution of morphologies during a spinodal phase separation of a ternary alloy with average composition $c_A = 0.45$, $c_B = 0.45$ and $c_C = 0.10$. Column $n_A(\mathbf{r}, t)$ represents the time evolution of the concentration profile of component A, column $n_B(\mathbf{r}, t)$ represents that of component B and column $n_C(\mathbf{r}, t)$ represents that of component C. Row a—reduced time $t^* = 5.0$; row b—$t^* = 20.0$; row c—$t^* = 50.0$; row d—$t^* = 100.0$.

β particles fall outside the three-phase region. Therefore, no γ phase particles are observed. It should be emphasized that the phase diagram of Fig. 1 is calculated for completely homogeneous phases whereas from the computer simulation, the alloy is inhomogeneous with interphase boundaries. Inhomogeneity can cause shift of phase boundaries.

SUMMARY

The nonequilibrium and highly nonlinear dynamics of spinodal phase separation in ternary alloys is investigated using a computer simulation technique based on a microscopic diffusion theory. Even though I chose a particular system with symmetric interactions among different species and the same kinetic coefficients for interatomic interchanges, the results obtained are generic to real ternary systems in terms of the morphological patterns and the sequence of phase transformations. For all the compositions investigated, there are at least a very short-time period in the beginning that the morphologies appear to be interconnected. Very often decomposition of a homogeneous alloy into a three-phase

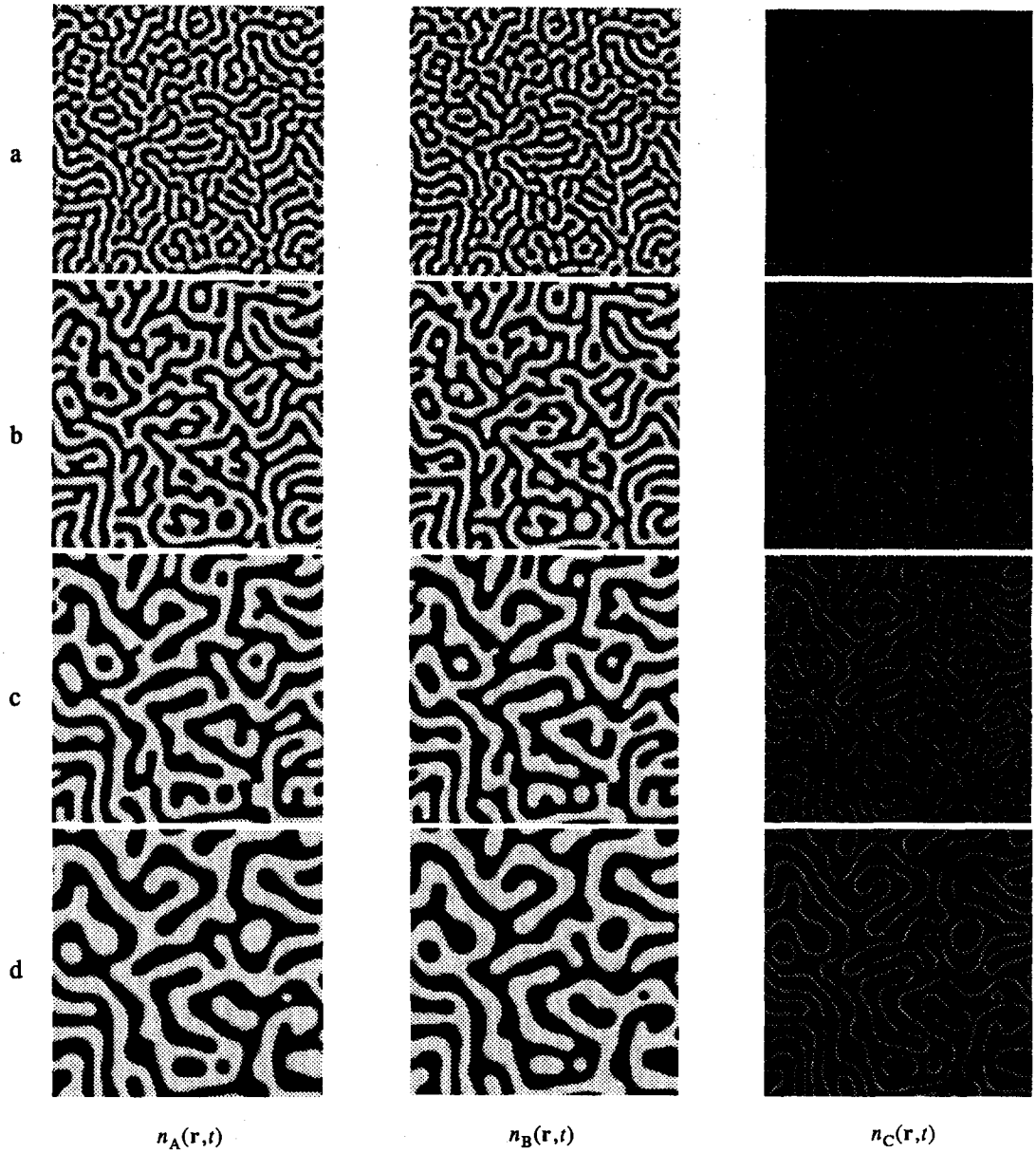

Fig. 7. Temporal evolution of morphologies during a spinodal phase separation of a ternary alloy with average composition $c_A = 0.495$, $c_B = 0.495$ and $c_C = 0.01$. Column $n_A(\mathbf{r}, t)$ represents the time evolution of the concentration profile of component A, column $n_B(\mathbf{r}, t)$ represents that of component B and column $n_C(\mathbf{r}, t)$ represents that of component C. Row a—reduced time $t^* = 10.0$; row b—$t^* = 20.0$; row c—$t^* = 50.0$; row d—$t^* = 100.0$.

mixture takes place in two different stages corresponding to the relaxation of the total free energy with respect to two conserved order parameters, i.e. two independent composition parameters for a ternary alloy. Interesting results on phase separation in isolated small regions were obtained (Fig. 4). It raises an important question how phase separation occurs in very small grains in a polycrystalline sample. It is expected that the interfaces of these small particles should play an important role, probably a dominant one, in the spinodal decomposition kinetics. It is shown that a third minor component added into a binary alloy strongly segregates to the interphase boundaries of a two-phase mixture during decomposition and subsequent coarsening (Fig. 7).

Acknowledgements—This work is supported by the ARPA/NIST program on Mathematical Modeling of Microstructure Evolution in Advanced Alloys and by NSF under the grant number DMR-9311898. The computing time is provided by the Pittsburgh Supercomputing Center under the grant number DMR-900022P. The author would like to thank Drs John Simmons, John Cahn and William Boettinger at NIST for useful suggestions and discussions. He is also grateful to Mr Yunzhi Wang at Rutgers University for his help in making those color pictures presented in this paper.

REFERENCES

1. J. W. Cahn and J. E. Hilliard, *J. Chem. Phys.* **28,** 258 (1958).
2. J. W. Cahn, *Acta metall.* **9,** 795 (1961).
3. J. E. Hilliard, in *Phase Transformations* (edited by H. I. Aronson). Am. Soc. Metals, Metals Park, Ohio (1970).
4. J. L. Meijering, *Philips Res. Rep.* **5,** 333 (1950); **6,** 183 (1951).
5. R. Kikuchi, *Acta metall.* **25,** 195 (1977).
6. R. Kikuchi, R., D. de Fontaine, M. Murakami and T. Nakamura, *Acta metall.* **25,** 207 (1977).
7. D. de Fontaine, *J. Phys. Chem. Solids* **33,** 297 (1972); *ibid.* **34,** 1285 (1973).
8. J. E. Morral and J. W. Cahn, *Acta metall.* **19,** 1037 (1971).
9. J. J. Hoyt, *Acta metall.* **37,** 2489 (1989).
10. J. S. Langer, *Ann. Phys.* **65,** 53 (1971); *Acta metall.* **21,** 1649 (1973).
11. J. J. Hoyt, *Acta metall.* **38,** 227 (1990).
12. A. G. Khachaturyan, *Fiz. tverd. Tela* **9,** 2595 (1967); *Sov. Phys. Solid State* **9,** 2040 (1968).
13. L. Q. Chen, *Scripta metall. mater.* **29,** 683 (1993).
14. L. Q. Chen and A. G. Khachaturyan, *Acta metall. mater.* **39,** 2533 (1991).